



# Room Temperature Magnetic Detection of Spin Switching in Nanosized Spin-Crossover Materials\*\*

Tran Quang Hung, Ferial Terki,\* Souleymane Kamara, Mourad Dehbaoui, Salam Charar, Brajalal Sinha, CheolGi Kim,\* Philippe Gandit, Il'ya A. Gural'skiy, Gabor Molnar, Lionel Salmon, Helena J. Shepherd, and Azzedine Bousseksou\*

Recently, nanoscale spin-crossover (SCO) particles have been the subject of great interest. The change in the 3d electronic configuration of the metal ion results in significant changes in the metal–ligand bond length and geometry, as well as in the molecular volume. Hence the spin switching process is accompanied by a remarkable change in the color, mechanical properties, dielectric properties, and magnetic susceptibility. The synthesis and investigation of these materials at reduced length scales is central not only to the exploration of fundamental effects of size reduction in these systems, but also for the development of new functional materials with applications, including guest molecule sensing, memory devices, and molecular switches.<sup>[1]</sup>

Until now, the observation of spin switching was essentially limited to the simple investigation of the temperature dependence of the magnetization or the optical absorption in a huge ensemble of nanoparticles with different degrees of size and shape dispersion. The development of methods for the detection of single SCO particles would thus be desirable not only from a fundamental perspective, but also for applications; however, such methods remain scarce.<sup>[2]</sup>

In the field of nanoscale magnetic measurements, the state of the art is the micro-superconducting quantum interference device (micro-SQUID) and the nano-SQUID, which allow the detection of magnetization reversal in a few magnetic nanoparticles (or even a single one) through their deposition directly onto the microbridge Josephson junctions. However, for low noise operation, the Josephson junctions are normally made of a low temperature superconducting material such as Nb, Ti/Al, or Pd/Al bilayers.<sup>[3]</sup> Thus far, the working temperature of the system was limited to below a few tens of Kelvin. Consequently, the conventional micro- or nano-SQUID technique is not appropriate for studying magnetic properties in the room-temperature range.

With a view towards measurement of the room temperature spin switching of a small quantity of SCO material (or even a single nanoparticle), herein we present a novel prototype based on low noise magnetoresistive (MR) micro-magnetometry. Compared to an actual ultrasensitive SQUID, our magnetoresistive SQUID-like prototype has significant advantages, including room temperature operation, reduced complexity of equipment, increased portability, and more flexible implementation. Furthermore, we can adjust the design of the sensors on the microscopic scale to optimize the sensitivity, so as to detect the nano- or pico-tesla local fields potentially generated by a single micro- or nano-object in the close vicinity of the sensor surface.<sup>[4]</sup> Such a device is well adapted to study spin switching or magnetic phase transitions in these molecular systems, which only induce low-flux variation in the room temperature range.

SCO nanoparticles of  $[\text{Fe}(\text{hptrz})_3](\text{OTs})_2$  ( $\text{hptrz}$  = 4-heptyl-1,2,4-triazole,  $\text{OTs}$  = *p*-toluenesulfonyl) were specifically synthesized for these experiments in homogenous solutions,<sup>[5]</sup> thus yielding a highly concentrated and redispersible nanoparticle powder without the presence of large amount of surfactants or other additives. Transmission electron microscopy (TEM) images of the SCO particles reveal a mean size of  $(250 \pm 40)$  nm (Figure 1). The transition temperatures of a large dehydrated ensemble of this nanoparticle powder are  $T_{1/2\downarrow} = 309$  K and  $T_{1/2\uparrow} = 315$  K in cooling and heating cycles, respectively.<sup>[5]</sup>

A highly sensitive hybrid MR sensor, which combines anisotropic magnetoresistive (AMR) and planar Hall effects (PHE),<sup>[6]</sup> was used for the detection of spin-state switching in SCO  $[\text{Fe}(\text{hptrz})_3](\text{OTs})_2$  nanoparticles. The devices were optimized based on a multi-ring architecture and a trilayer structure Ta/NiFe/Cu/IrMn/Ta (3, 20, 0.2, 10, 3 nm, respectively). In this structure, a soft magnetic layer of NiFe is the


[\*] Dr. T. Q. Hung, Dr. F. Terki, Dr. S. Kamara, M. Dehbaoui, Prof. S. Charar  
Laboratoire Charles Coulomb, CNRS-UM2, University Montpellier 2, PEPS Team, Place Eugène Bataillon, 34095 Montpellier Cedex 05 (France)  
E-mail: ferial.terki@univ-montp2.fr

B. Sinha, Prof. C. G. Kim  
Center for NanoBioEngineering and Spintronics  
Chungnam National University  
220 Gungdong, Yuseong-gu, 305-764 Daejeon (South Korea)  
E-mail: cgkim@cnu.ac.kr

Dr. P. Gandit  
Institut Neel CNRS/MCBT UPR2940  
38042 Grenoble, cedex 9 (France)

I. A. Gural'skiy, Dr. G. Molnar, Dr. L. Salmon, Dr. H. J. Shepherd, Dr. A. Bousseksou  
CNRS UPR-8241, and Université de Toulouse  
UPS, INP, Toulouse (France)  
E-mail: azzedine.bousseksou@lcc-toulouse.fr

[\*\*] We acknowledge financial support from EADS Corporate Foundation (to F.T.), MEST World-Class University program through the NRF (R32-20026 to C.G.K.), and CROSSNANOMAT (ANR-10-BLAN-0716 to A.B.). C. Consejo, P. Solignac, and O. Kraieva are thanked for their technical assistance.

 Supporting information for this article is available on the WWW under <http://dx.doi.org/10.1002/anie.201205952>.

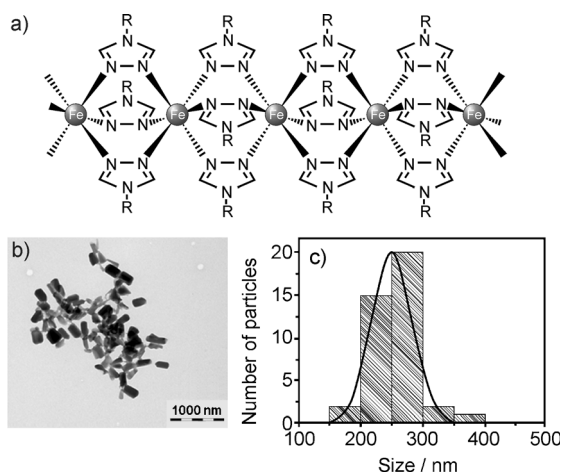


**Figure 1.** a) Polymeric 1D-chain structure of  $[\text{Fe}(\text{hptrz})_3]$ , b) TEM image of  $250 \pm 40$  nm nanoparticles and c) the corresponding size histogram (largest dimension of each nanoparticle used for statistics).

sensing material; it is weakly exchange-coupled to an antiferromagnetic layer (IrMn) through a few atomic layers of Cu for thermal stability. This multilayer stack has very high sensitivity and low noise for a sensor material. In this prototype, the sensor has a sensitivity of ca.  $S = 15 \text{ V T}^{-1}$  and a low white noise of ca.  $1 \text{ nV Hz}^{-1/2}$  at 100 Hz. The sensor materials, measurement, and calibration methods are described in detail elsewhere.<sup>[7]</sup> To prevent both the leakage of solution and contamination, the sensor surface is passivated by a  $\text{Si}_2\text{O}_3/\text{Si}_3\text{N}_4$  bilayer with a nominal thickness of 200 nm.

In this experiment, the chloroform suspension of  $[\text{Fe}(\text{hptrz})_3](\text{OTs})_2$  nanoparticles is directly dropped onto the whole active surface of the sensor. The measurement was carried out under an external magnetic field of 1.4 mT. The sensor detects the magnetic signature of the diamagnetic-to-paramagnetic phase transition by means of a full Wheatstone bridge configuration.<sup>[8]</sup>

Figure 2 shows a measured voltage profile of the micromagnetometer as a function of temperature with SCO

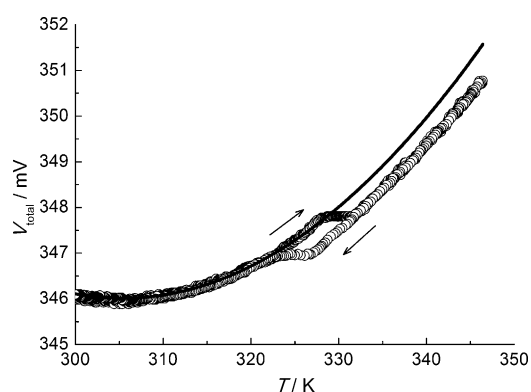


**Figure 2.** The measured voltage of the micromagnetometer with SCO particles on the surface as a function of temperature. The direction of the arrows shows the voltage response for increasing and decreasing temperatures. Experimental voltage ( $\circ$ ), fitting drift voltage ( $\text{—}$ ).

nanoparticles on its surface. This voltage profile ( $V_{\text{total}}$ ) contains two contributions: a concave variation of the voltage drift ( $V_{\text{drift}}$ ) of the micromagnetometer and a voltage response caused by the spin switching of the SCO particles ( $V_{\text{stray}}$ ) [Eq. 1].

$$V_{\text{total}} = V_{\text{drift}} + V_{\text{stray}} \quad (1)$$

The SCO of particles is clearly observed in Figure 2, which shows the temperature dependence of the measured voltage. After subtraction of the voltage drift (for details see the Supporting Information, S1), just the voltage response caused by the spin switching of the SCO particles remains, as shown in Figure 3a. From this, the spin-switching temperatures are estimated to be approximately  $T_{1/2\downarrow} = 325 \text{ K}$  and  $T_{1/2\uparrow} = 331 \text{ K}$  in the cooling and heating cycles, respectively.

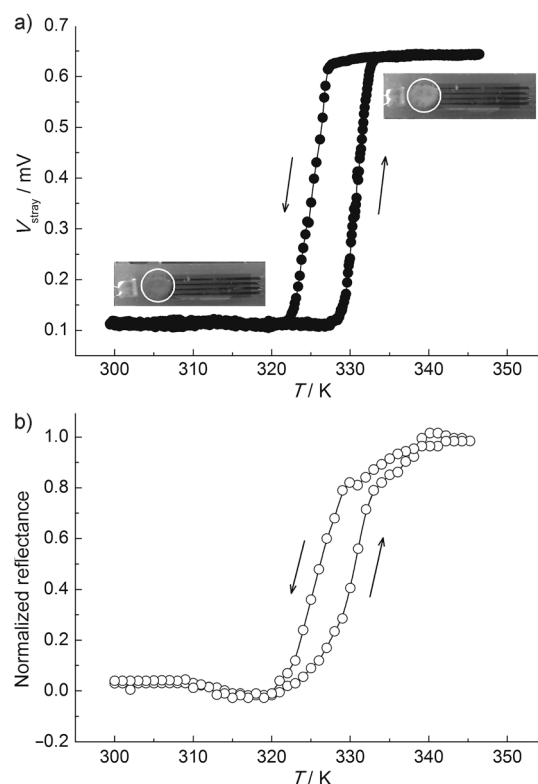


**Figure 3.** a) The voltage change associated with the spin transition of  $[\text{Fe}(\text{hptrz})_3](\text{OTs})_2$  nanoparticles. The diamagnetic and paramagnetic phases are characterized by lower and higher voltage, respectively. The insets show the color change of the particles: pink in the diamagnetic low spin state and white in the paramagnetic high spin state. b) Reflectance measurements ( $\lambda = (550 \pm 20) \text{ nm}$ ) of the particles on the sensor surface.

The spin transition of the nanoparticles deposited on the device was also followed by the change in optical reflectance induced by the (dis)appearance of the d–d absorption band of the SCO complex (centered at 550 nm) between 300 and 345 K, as shown in Figure 3b. The observed SCO transition temperatures are in good agreement with those deduced from magnetic measurements.

We should mention that the transition temperatures in these measurements are different from those reported in reference [5] ( $T_{1/2\downarrow} = 309$  K and  $T_{1/2\uparrow} = 315$  K). This is due to the different sample environment of the two measurement setups: the measurements in reference [5] were performed in a dry  $N_2$  atmosphere, whereas the micromagnetometry voltage and reflectance measurements presented here were recorded in open air. As shown in the Supporting Information (S2), the transition temperature measured by the micromagnetometry device is very sensitive to the humidity of the sample environment due to the hygroscopic nature of these particles.

In the following we will evaluate 1) the volume of the particles used in this experiment and 2) the minimum number of particles that the sensor could detect. The ultimate challenge is to improve the sensitivity to achieve single particle detection by optimizing the novel MR prototype and the particle size. In the high spin state, particles under an external magnetic field will produce a stray field. As a first approximation, we can assume that the stray fields from different particles do not interact with each other. The stray field of a particle at a distance  $r$  is described as follows:<sup>[9]</sup>

$$\hat{H}_{\text{stray}} = \frac{MR^3}{3r^3} (3(\hat{M}\hat{r})\hat{r} - \hat{M}) \quad (2)$$

Here,  $M$  is the magnetization,  $R$  is the mean radius of the SCO particle, and  $r$  is the distance from the particle to the measurement point. This stray field causes the change of sensor voltage, which can be estimated by the following equation (see also the Supporting Information, S3).

$$V_{\text{stray}} = H_{\text{stray}}S = -\frac{SR^3\chi_v H}{3z_o^3(1 + \frac{R^2}{z_o^2})^{3/2}} \quad (3)$$

Here, the negative sign means that the stray field reduces the sensor voltage.  $S$  and  $\rho_s$  are the sensitivity and the radius of the sensor element, respectively;  $H$  is the applied field,  $z_o$  is the distance from the particle to the sensing layer. In this calculation we assumed that the particles (spherical shape with an average diameter of 250 nm) are placed directly on top of the sensor surface under an applied field of 1.4 mT. The measured sensor sensitivity ( $S$ ) is approximately  $15 \text{ VT}^{-1}$ , which is deduced from the voltage profile of the sensor ( $S = dV/dH$ ). The diameter of the sensor element is 300  $\mu\text{m}$ . The volume susceptibility in the high spin state of the particles ( $\chi_v$ ) is calculated to be ca.  $4.2 \times 10^{-4}$  (Supporting Information, S4).

By substituting these values into equation (3), the  $V_{\text{stray}}$  induced by one particle is  $-3 \times 10^{-5}$  nV. From the deduced  $V_{\text{stray}}$  (Figure 3a), the volume of the detected particles in our experiment is estimated to be ca.  $3 \times 10^{-3} \text{ mm}^3$ . Based on our measurements the sensor noise is ca. 1 nV, thus the minimal voltage that can be detected by our setup is ca. 5 nV (signal-to-noise = 5), which corresponds to the voltage signal generated by one monolayer with 13 % particle coverage. In other words, the detection limit of the sensor is a particle volume of  $2 \times 10^{-6} \text{ mm}^3$ . It is noteworthy that no signal for this quantity of sample can be detected in a commercially available SQUID magnetometer. For example, a high-end

commercial magnetometer<sup>[10]</sup> with a sensitivity of  $10^{-8}$  emu at 1000 Oe, could only detect a minimum particle volume of about  $5 \times 10^{-2} \text{ mm}^3$ .

Furthermore, the detection capability of our MR magnetometer strongly depends on the sensor area, as expressed in Equation 3. Consequently, by reducing the sensor size to 300 nm and the passivation layer thickness to ca. 100 nm, a single 250 nm particle with a volume susceptibility of  $4.2 \times 10^{-4}$  will generate a voltage response of 5.4 nV. In this estimation, we consider the sensitivity to be  $0.01 \text{ VT}^{-1}$  because of the small sensor size and an applied field of 1.4 mT. According to this quantitative estimation, we believe that in the near future we should be able to develop an optimized nanoscale device to detect the magnetic signature of the spin transition of a single SCO nanoparticle.

In conclusion, we have implemented a novel prototype for a SQUID-like magnetometry device for the indirect detection of room temperature switching in an SCO nanoparticle. In this work, an ensemble of  $[\text{Fe}(\text{hptrz})_3](\text{OTs})_2$  nanoparticles with a volume of ca.  $3 \times 10^{-3} \text{ mm}^3$  has been investigated and was found to give rise to a voltage signal of about 5.5  $\mu\text{V}$  (0.55 mV after amplification in Figure 3a). Further improvements to the device are in progress, such as the enhancement of sensitivity, reducing noise, and the implementation of a new concept based on a differential method for a more accurate signal detection, which increases the sensitivity by a factor of four. This optimization should provide us with an original device for detecting the room-temperature spin switching of a few nanoparticles and, ultimately, a single particle. This work serves as a proof of concept for this novel micromagnetometry approach; the substantial and significant benefits of this approach over conventional SQUID (significantly increased sensitivity for detection of low quantities of nanoparticles) and nano-SQUID (room temperature operation) techniques have been highlighted. Both of these developments represent significant breakthroughs within the field of molecular magnetism. Efforts towards detecting SCO in single objects at around room temperature using this powerful method in differential mode are on-going.

## Experimental Section

The  $[\text{Fe}(\text{hptrz})_3](\text{OTs})_2$  nanoparticles were synthesized in a homogeneous medium in the presence of polyethylene glycol (PEG-400) as a stabilizing agent.<sup>[5]</sup> Two distinct solutions were prepared: 1) Iron(II) tosylate hexahydrate (30 mg, 0.06 mmol, 1 equiv), ascorbic acid (1 mg), and PEG-400 (200  $\mu\text{L}$ ) in water (2 mL); 2) hptrz (30 mg, 0.18 mmol, 1 equiv) in water (2 mL). The two solutions were rapidly mixed. The mixture becomes turbid in a few seconds, followed by the formation of a pink precipitate. TEM measurements were used to characterize the size of the nanoparticles.

The setup to detect the spin switching of SCO nanoparticles is illustrated in Figure 4a. The temperature of the sample varies from 300 to 350 K, and is controlled by a Lakeshore 332 temperature controller. The whole system is placed under an alternating and a continuous magnetic field ( $H_{AC}$  and  $H_{DC}$ ) with an angle of 20 degrees between the easy axis of the sensor and the magnetic field direction. With this combination of both  $H_{AC}$  and  $H_{DC}$  fields, the sensitivity of the prototype sensor is maximized. The voltage signal is measured by a lock-in amplifier after magnification by a factor of 100.

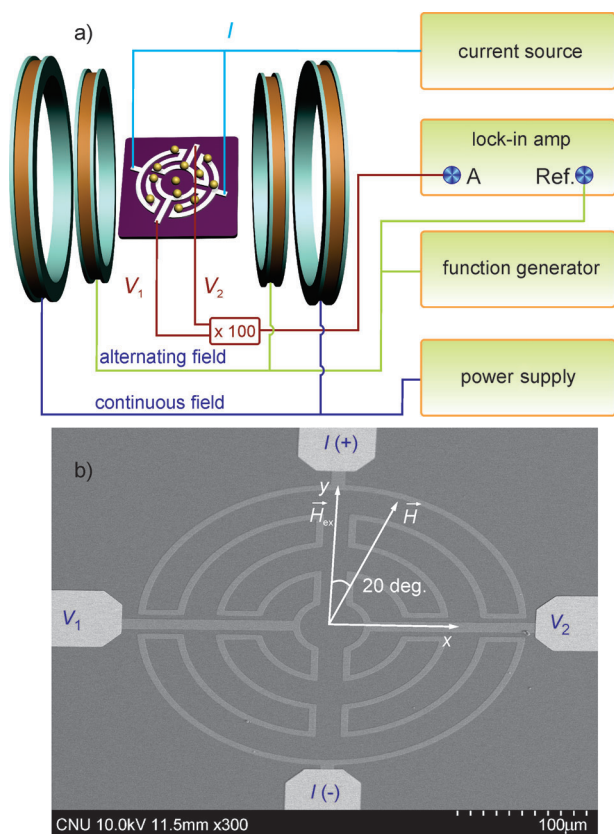


**Figure 4.** a) Experimental setup of the micromagnetometer for detection of SCO nanoparticles. The particles are dropped on the whole surface of the magnetometer. The AC and DC fields are generated from two pairs of Helmholtz coils. The operating DC current is applied to the sensor and its sensor output voltage caused by the AC field is measured by a lock-in amplifier. b) SEM image of a sensor junction, showing the current and voltage electrodes, applied field, and exchange-coupled field direction.

Figure 4b shows an SEM image of a representative 300  $\mu\text{m}$  multi-ring sensor junction, where the two pairs of electrodes, for applying current and measurement voltage, are perpendicular. The direction of the current electrodes is parallel to the exchange-coupled field direction (the easy axis of the sensor). The exchange-coupled field ( $H_{\text{ex}}$ ) of the sample is ca. 2 mT.

Received: July 25, 2012

Published online: December 11, 2012

**Keywords:** magnetic properties · micro-squid-like devices · room temperature detection · spin crossover

- [1] A. Bousseksou, G. Molnár, L. Salmon, W. Nicolazzi, *Chem. Soc. Rev.* **2011**, 40, 3313.
- [2] a) G. Molnár, S. Cobo, J. A. Real, F. Carcenac, E. Daran, C. Vieu, A. Bousseksou, *Adv. Mater.* **2007**, 19, 2163–2167; b) C. Arnaud, T. Forestier, N. Daro, E. Freysz, J.-F. Létard, G. Pauliat, G. Roosen, *Chem. Phys. Lett.* **2009**, 470, 131–135; c) F. Prins, M. Monrabal-Capilla, E. A. Osorio, E. Coronado, H. S. J. van der Zant, *Adv. Mater.* **2011**, 23, 1545–1549; d) C. M. Quintero, I. A. Gural'skiy, L. Salmon, C. Bergaud, G. Molnár, A. Bousseksou, *J. Mater. Chem.* **2012**, 22, 3745–3751.
- [3] a) M. Jamet, W. Wernsdorfer, C. Thirion, D. Mailly, V. Dupuis, P. Melinon, A. Perez, *Phys. Rev. Lett.* **2001**, 86, 4676–4679; b) W. Wernsdorfer, E. Bonet Orozco, K. Hasselbach, A. Benoit, B. Barbara, N. Demoncey, A. Loiseau, D. Boivin, H. Pascar, D. Mailly, *Phys. Rev. Lett.* **1997**, 79, 4014–4017; c) A. Finkler, Y. Segev, Y. Myasoedov, M. L. Rappaport, L. Ne'eman, D. Vasyuko, E. Zeldov, M. E. Huber, J. Martin, A. Yacoby, *Nano Lett.* **2010**, 10, 1046–1049; d) P. Jarillo-Herrero, J. A. van Dam, L. P. Kouwenhoven, *Nature* **2006**, 439, 953–956; e) J.-P. Cleuziou, W. Wernsdorfer, V. Bouchiat, T. Ondarcuhuand, M. Monthieux, *Nat. Nanotechnol.* **2006**, 1, 53–59.
- [4] a) M. Pannetier, C. Fermon, G. Le Goff, J. Simola, E. Kerr, *Science* **2004**, 304, 1648–1650; b) Z. Marinho, S. Cardoso, R. Chaves, R. Ferreira, L. V. Melo, P. P. Freitas, *J. Appl. Phys.* **2011**, 109, 07E521; c) A. Persson, R. Bejhed, H. Nguyen, K. Gunnarsson, B. T. Dalslet, F. W. Østerberg, M. F. Hansen, P. Svedlindh, *Sens. Actuators A* **2011**, 171, 212–218.
- [5] Sample 8 as reported in: I. A. Gural'skiy, C. M. Quintero, G. Molnár, I. O. Fritsky, L. Salmon, A. Bousseksou, *Chem. Eur. J.* **2012**, 18, 9946.
- [6] a) S. J. Oh, P. B. Patil, T. Q. Hung, B. H. Lim, M. Takahashi, D. Y. Kim, C. G. Kim, *Solid State Commun.* **2011**, 151, 1248–1251; b) T. Q. Hung, S. J. Oh, B. Sinha, J.-R. Jeong, D.-Y. Kim, C. G. Kim, *J. Appl. Phys.* **2010**, 107, 09E715; c) T. Q. Hung, J.-R. Jeong, D. Y. Kim, N. H. Duc, C. G. Kim, *J. Phys. D* **2009**, 42, 055007.
- [7] a) T. Q. Hung, D. Y. Kim, B. Parvatheeswara Rao, C. G. Kim, in: *State of the Art in Biosensors*, Book 1, (T. Rinken, Ed.), Intech, **2012**, DOI: 10.5772/52820; b) F. Terki, T. Q. Hung, B. Sinha, C. G. Kim, I. Gural'skiy, G. Molnár, L. Salmon, A. Bousseksou, submitted for EU patent, **2012**, reg. EP12305852.1.
- [8] a) C. Reig, M. D. Cubells-Beltran, D. Ramirez Munoz, *Sensors* **2009**, 9, 7919–7942; b) K. Hoffmann, *Applying the Wheatstone bridge circuit*, HBM S1569-1.1en, HBM, Darmstadt, Germany.
- [9] R. C. O'Handley, *Modern Magnetic materials: Principle and applications*, Wiley, New York, **2000**, pp. 53–55.
- [10] C. D. Graham, *J. Mater. Sci. Technol.* **2000**, 16, 97–101.